Photon-photon resonance enhanced modulation bandwidth in CCIG lasers

Photon-Photon Resonance Enhanced Modulation Bandwidth in CCIG lasers

M. Vallone, P. Bardella and I. Montrosset
Dipartimento di elettronica, Politecnico di Torino, Turin, Italy

Introduction

The possibility to use higher longitudinal modes, exploiting a photon-photon resonance (PPR) to obtain Extended Modulation Bandwidth (EMB) operation has been already studied both theoretically and experimentally, for DFB, DBR and in multi-section lasers such as Coupled Cavity Injection Gratings [1-5].

In this work we present a systematic procedure to find EMB condition that we applied to all the previous cases and we report here the application to a CCIG laser composed by two cavities (active and passive) separated by a grating section. The occurrence of this condition has been explored by varying the refractive index of the passive sections and evaluating the mode spacing between the lasing mode and the adjacent ones with a static model program. In this way, the conditions to obtain PPR are found exploiting the compound cavity interference effects. Successively we verified the occurrence of these conditions using a Finite Difference Time Domain (FDTD) dynamic model [6].

Static model

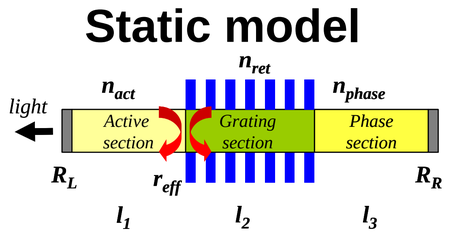

Fig. 1. Model schematics.: left, for an arbitrary number of sections, right, for a 3-sections CCIG

The static model for the 3-sections CCIG in Fig.1 is based on coupled modes equation relating the slow varying components of the co-propagating and contra-propagating fields in each section. The resonance conditions reads:

$$G = \bar{r}_L \; e^{-2i\beta_3 l_3}\left[\frac{(T_{11})^2\,\vec{r}_R\; e^{-2i(\beta_{02}l_2+\beta_1 l_1)}+(T_{12})^2}{(T_{21})^2\,\vec{r}_R\; e^{-2i(\beta_{02}l_2+\beta_1 l_1)}+(T_{22})^2}\right] = |G|e^{i\varphi},$$

$$\varphi_n = \operatorname{atan}\left(\frac{\mathrm{Im}(G)}{\mathrm{Re}(G)}\right) = 2\pi n,\; n=1,2,\ldots \quad \text{for the lasing mode } n=m,\; |G_m|=1,\; \varphi_m = 2m\pi$$

for the non-lasing modes $n\neq m$ $\quad |G_n|<1,\; (g_m,\varphi_n)$

where T_{ij} is the grating section transfer matrix. For the lasing mode $n=m$, $|G_m|=1$ and $\varphi_m=2m\pi$. For the side modes $n\neq m$, $|G_n|<1$ and $\varphi_n=2n\pi$.

In Fig. 2 it is reported an example of EMB condition for a CCIG having a grating with coupling coefficient κ = 20 cm^{-1} and l_2= 400 μm, and with 100 μm long active and phase sections.The material is a multi-quantum-well structure emitting around 1550 nm. The grating section is tuned with injection, changing its $n_{eff,grat}$ in order to achieve the PPR condition. The solution plots are shown in Fig. 2. The lasing and the competing mode (indicated any an arrow) belong to a 3-fold degenerate solution and the lasing mode operates in detuned loading condition [1].

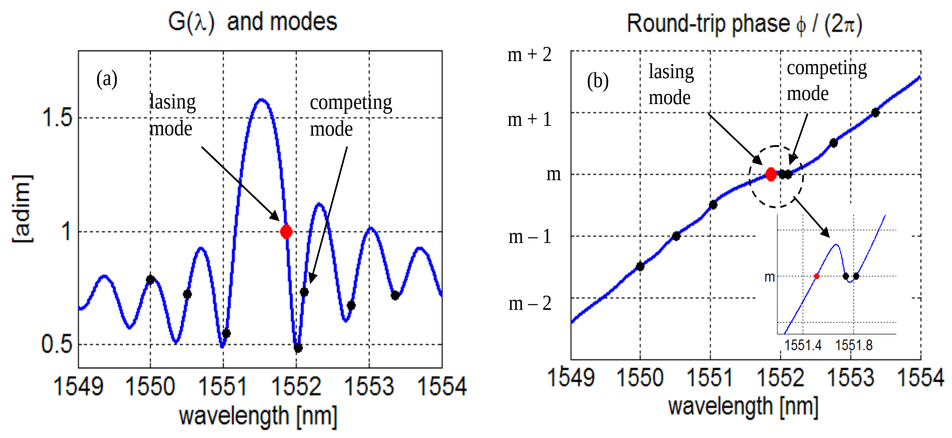

Fig. 2. Round-trip gain G (a) and phase (b) versus wavelength. Spots and arrows indicate the lasing and the competing modes. In the inset of (b), the detail of the feature responsible of the PPR is shown.

Varying the effective indices in 2 of the 3 sections, we may build color-plot of frequency separation between the lasing mode and the closest competing one on the long-wavelength side of the spectrum), in order to find conditions suitable for PPR. An example for the structure described above is shown in Fig. 3.

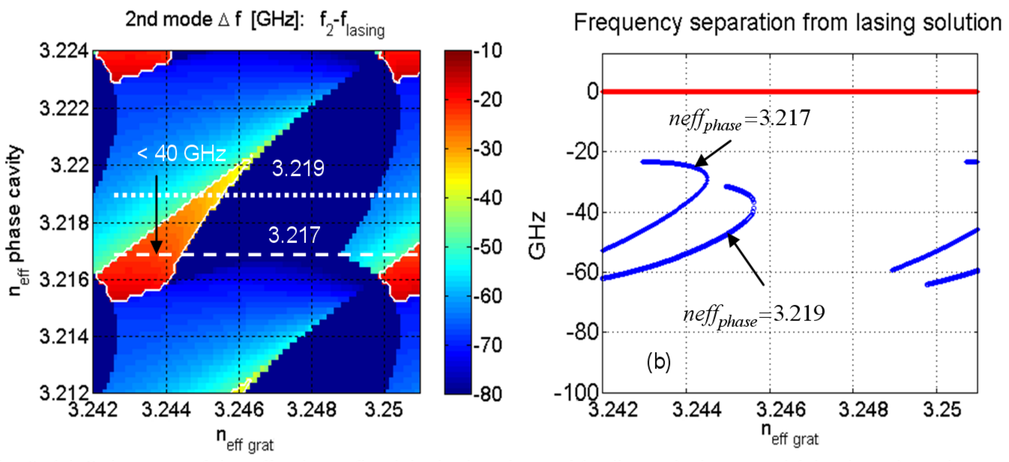

Fig. 3. (a) Color-map of the effective reflectivity in the plane of (ordinates) phase and (abscissas) grating section effective index $n_{eff,grat}$. Inside the red region marked by a white contour, frequency separation between the lasing and the first competing mode (on the long-wavelength side of the spectrum) is below 40 GHz.
(b) The frequency separation as defined above is plotted versus $n_{eff,grat}$, for two cuts in the plane of Fig. 3(a), as indicated by the two dotted and dashed white lines.

Having found these conditions in short CPU time, the more time-consuming ***Time-Domain Travelling-Wave model*** can then be used to investigate the CCIG dynamical properties.

Time-Domain Travelling-Wave model

A time domain, travelling wave (TDTW) model was used in order to validate the static model and to investigate the dynamic behaviour of the considered device. This model considers the slowly varying envelop of the forward and backward propagating fields [5]; the set of wave equations

$$\left[\frac{\partial}{\partial z}\pm\frac{1}{v_g}\frac{\partial}{\partial t}\right]R^{\pm}(z,t)=\left\{\Gamma_{xy}g(N)-\alpha_0-j\frac{\omega_0}{c}\left[n_{eff}(N,z)-n_{eff,0}\right]\right\}R^{\pm}(z,t)\mp j\tilde{\kappa}^{\pm}R^{\mp}(z,t)+S_{sp}(t,z)$$

is solved using the finite difference method with the split-step algorithm [6].
Carrier concentration is described trough a rate equation:

$$\frac{d}{dt}N(z,t)=\frac{I(t)}{eV}-\frac{N(z,t)}{\tau(N)}-\frac{2v_g g(N)S(z,t)}{1+\varepsilon S(z,t)} \quad \text{with} \quad S(z,t)=\left|R^{+}(z,t)\right|^2+\left|R^{-}(z,t)\right|^2$$

while gain dispersion is introduced using a numerical IIR filter [7] that reproduces the same wavelength dependence introduced in the static model.
Fig. 4(a) shows the position of the cavity modes

- calculated with the static model (continuous curves),
- extracted from the TDTW spectra simulated for an injected current of 2I_{th}

for different values of $n_{eff,grat}$.
Results are consistent; an efficient PPR appear possible when $n_{eff,grat}$ is around 3.246 where the frequency separation between the lasing mode and its closest neighbour is around 33GHz.

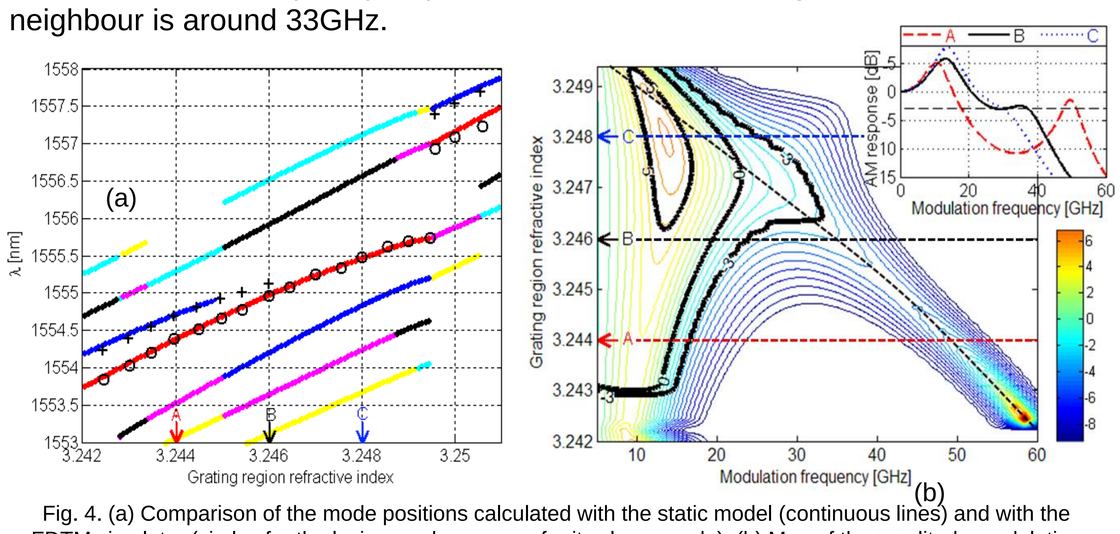

Fig. 4. (a) Comparison of the mode positions calculated with the static model (continuous lines) and with the FDTM simulator (circles for the lasing mode, crosses for its closer mode); (b) Map of the amplitude modulation responses calculated at 2I_{th} for different values of the grating effective refractive index. Inset: cuts of the map reporting the AM responses when $n_{eff,grat}$=3.244 (A), $n_{eff,grat}$=3.246 (B), and $n_{eff,grat}$=3.248 (C).

Amplitude modulation (AM) responses of the device were then calculated and reported in a map in the in the $n_{eff,grat}$ - modulation frequency plane (Fig. 4b).
The following situations appear, for increasing values of $n_{eff,grat}$:

- initially ($n_{eff,grat}$ ≈3.2425), a strong PPR resonance peak appears at 58 GHz; the device is self-pulsating;
- around (A), self-pulsations disappear; the frequency separation between the lasing mode and its closest neighbour reduces but it is still so high that a large dip is present in the AM response;
- near (B), the gap between the two resonance peaks is finally closed, leading to a -3dB bandwidth larger than 33 GHz;
- finally, when the two modes merge (C), a single strong modulation peak is obtained with reduction of the resulting -3dB modulation bandwidth.

Fig. 5(a-b) show the eye diagrams obtained by a large signal modulation of the CCIG at the maximum EMB small signal modulation condition. The applied current represents a NRZ PRBS signal and ranges from 45 mA (bit 0) to 100 mA (bit 1); 4dB extinction ration is obtained with a 33 Gb/s modulation.

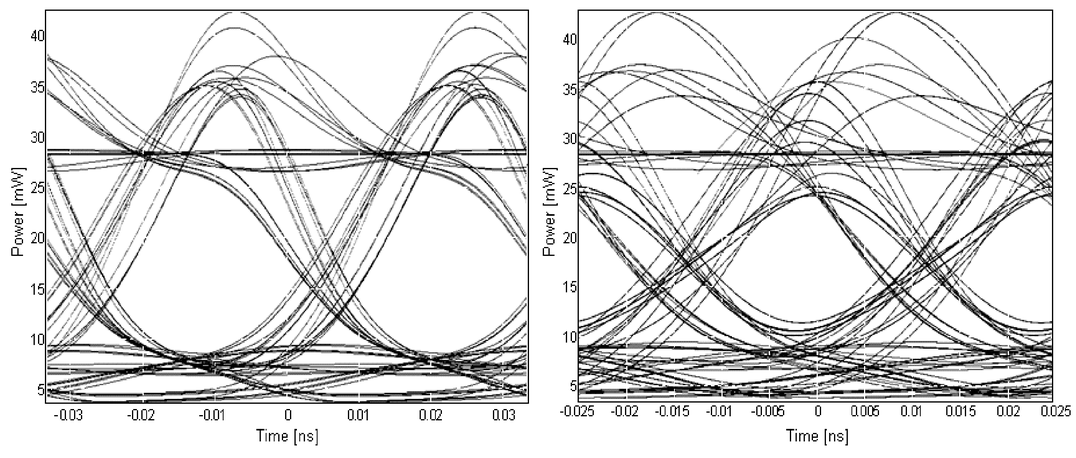

Fig. 5. Eye diagrams calculated at the optimal EMB condition ($n_{eff,grat}$=3.246) with a NRZ PRBS signal with 33-Gbit/s (a) and a 40-Gbit/s (b) bit rate.

Conclusions

Two complementary models have been proposed to search for EMB operation. First, a static analysis of the laser cavity modes allows finding proper PPR conditions, then with FDTW the condition for EMB is verified by computing both the small and large signal modulation responses. As an example, we reported the results obtained for a CCIG laser where a fine-tuning of the device parameters allowed obtaining a -3dB EMB of around 33GHz.

The research leading to these results has received funding from the European Community's Seventh Framework Programme under grant agreement n° 224366 (Delight project).

References

[1] G. Mortier et al., IEEE J. Quantum Electron., vol. 36, n. 12, Dec. 2000
[2] U. Feiste, IEEE J. Quantum Electron., vol. 34, n. 12, Dec. 1998
[3] M. Radziunas et al., IEEE J. Sel. Top. Quantum Electron., vol. 13, 2007
[4] U. Troppenz et al., EOS Annual Meeting 2008
[5] W. Kaiser et al., IEEE Photon. Technol. lett., vol. 16, n. 9, Sept. 2004
[6] P. Bardella et al., IEEE J. Sel. Top. Quantum Electron., vol. 11, 2005
[7] D. J. Jones et al., IEEE J. Quantum Electron., vol. 31, n. 6, Jun. 1995